Locally controlled inhibitory mechanisms are involved in eukaryotic GPCR-mediated chemosensing

Xuehua Xu,[1] Martin Meier-Schellersheim,[2] Jianshe Yan,[1] and Tian Jin[1]

[1]Chemotaxis Signal Section, Laboratory of Immunogenetics, National Institute of Allergy and Infectious Diseases, National Institutes of Health, Rockville, MD 20852
[2]Program in Systems Immunology and Infectious Disease Modeling, Laboratory of Immunology, National Institute of Allergy and Infectious Diseases, National Institutes of Health, Bethesda, MD 20892

G protein–coupled receptor (GPCR) signaling mediates a balance of excitatory and inhibitory activities that regulate *Dictyostelium* chemosensing to cAMP. The molecular nature and kinetics of these inhibitors are unknown. We report that transient cAMP stimulations induce PIP_3 responses without a refractory period, suggesting that GPCR-mediated inhibition accumulates and decays slowly. Moreover, exposure to cAMP gradients leads to asymmetric distribution of the inhibitory components. The gradients induce a stable accumulation of the PIP_3 reporter PH_{Crac}-GFP in the front of cells near the cAMP source. Rapid withdrawal of the gradient led to the re-association of G protein subunits, and the return of the PIP_3 phosphatase PTEN and PH_{Crac}-GFP to their pre-stimulus distribution. Reapplication of cAMP stimulation produces a clear PH_{Crac}-GFP translocation to the back but not to the front, indicating that a stronger inhibition is maintained in the front of a polarized cell. Our study demonstrates a novel spatiotemporal feature of currently unknown inhibitory mechanisms acting locally on the PI3K activation pathway.

Introduction

Eukaryotic cells can detect and move up concentration gradients of chemoattractants, a process known as chemotaxis (Zigmond, 1978; Chung et al., 2001a; Iijima et al., 2002; Van Haastert and Devreotes, 2004). This behavior plays an important role in a number of processes, including metastasis, angiogenesis, immune responses, and inflammation (Murphy, 1994; Parent and Devreotes, 1999; Condeelis et al., 2005). Furthermore, chemotaxis is essential for cell aggregation in the life cycle of the social amoebae, *Dictyostelium discoideum* (Gerisch, 1982; Devreotes and Zigmond, 1988; Devreotes, 1994; Van Haastert and Devreotes, 2004). Chemotaxis is a coordinated phenomenon of three fundamental cell processes: gradient sensing, cell polarization, and cell motility. Chemotactic cells, such as neutrophils and *D. discoideum*, display polarized morphology, involving asymmetric distributions of many signaling molecules (Parent and Devreotes, 1999; Comer and Parent, 2002; Iijima et al., 2002; Devreotes and Janetopoulos, 2003), and heightened responsiveness to the attractant at their leading edge (Parent et al., 1998; Jin et al., 2000; Xu et al., 2003). These crawling cells extend their leading edges by assembling a force-generating network of actin filaments beneath the plasma membrane (Chung et al., 2001a; Pollard and Borisy, 2003). Elsewhere in the cell, actin collaborates with myosin to retract the rear of the advancing cell and to prevent errant pseudopod extension (Chung et al., 2001a). Consequently, the actin-depolymerizing agent Latrunculin can be used to eliminate polarization and motility of *D. discoideum* cells, and thus facilitate quantitative spatiotemporal analyses of the mechanisms underlying gradient sensing (Parent et al., 1998; Jin et al., 2000; Xu et al., 2005).

Gradient sensing is mediated by G protein–coupled receptors (GPCRs) and associated signaling components that detect the spatiotemporal changes of chemoattractants and translate shallow gradients of chemoattractants into steep intracellular gradients of signaling components (Parent and Devreotes, 1999; Chung et al., 2001b; Funamoto et al., 2002; Iijima et al., 2002). Binding of cAMP to the GPCR cAR1 induces the dissociation of heterotrimeric G proteins into Gα2 and Gβγ subunits (Jin et al., 2000; Janetopoulos et al., 2001; Xu et al., 2005). Free Gβγ activates Ras, thereby leading to the activation of PI3K, which converts $PI(4,5)P_2$ (PIP_2) to $PI(3,4,5)P_3$ (PIP_3) in the plasma membrane (Li et al., 2000; Funamoto et al., 2001; Stephens et al., 2002; Sasaki et al., 2004; Wessels et al., 2004). The phosphatase PTEN acts as an antagonist of PI3K, dephosphorylating

Correspondence to Tian Jin: tjin@niaid.nih.gov

Abbreviations used in this paper: CRAC, cytosolic regulator of adenylyl cyclase; GPCR, G protein–coupled receptor; PH, pleckstrin homology; WT, wild type.

The online version of this article contains supplemental material.

The Journal of Cell Biology, Vol. 178, No. 1, July 2, 2007 141–153
http://www.jcb.org/cgi/doi/10.1083/jcb.200611096

PIP_3 to regenerate PIP_2 (Funamoto et al., 2002; Iijima and Devreotes, 2002; Li et al., 2005). PIP_3 mediates cellular processes by recruiting proteins with pleckstrin homology (PH) domains, such as cytosolic regulator of adenylyl cyclase (CRAC) and Akt/PKB, to the plasma membrane (Parent et al., 1998; Meili et al., 1999). Both CRAC and Akt/PKB play roles in the regulation of actin polymerization during chemotaxis (Meili et al., 1999; Comer et al., 2005). Recent progress in fluorescence microscopy has permitted measurements of the spatiotemporal changes of many signaling events in living cells with high spatiotemporal resolution required to test models of gradient sensing (Ueda et al., 2001; Sasaki et al., 2004; Xu et al., 2005).

There are several key features of gradient sensing. First, cells have the ability to spontaneously terminate responses under a sustained cAMP stimulation in a process called "adaptation" (Parent et al., 1998; Xu et al., 2005). Second, if cAMP is removed from adapted cells, the cells will enter a de-adaptation phase—a refractory period lasting several minutes during which the cells progressively regain their ability to respond to another cAMP stimulation (Dinauer et al., 1980a,b). Third, cells have the capability of translating shallow cAMP gradients across the cell diameter into highly polarized intracellular responses, a process called "amplification" (Parent and Devreotes, 1999; Servant et al., 2000; Chung et al., 2001a). To explain these features, it has been proposed that an increase in receptor occupancy activates two antagonistic signaling processes: a rapid "excitation" that triggers cell responses, such as the membrane accumulation of PIP_3, and a slower "inhibition" that turns off those responses (Parent and Devreotes, 1999). Although many of the molecular mechanisms of the excitatory process have been identified, those of the inhibitory process have remained elusive.

The dynamic relationship between excitation and inhibition that leads to activation, adaptation, and amplification has been studied by direct visualization and quantitative analysis of the spatiotemporal changes in receptor occupancy, G protein dissociation, PI3K and PTEN distribution, and PIP_3 level along the membrane (Xu et al., 2005; Meier-Schellersheim et al., 2006). Over the years, models have been proposed to explain how the excitatory and the inhibitory processes interact in cells responding to chemoattractants to achieve adaptation or amplification (Meinhardt, 1999; Parent and Devreotes, 1999; Postma and Van Haastert, 2001; Devreotes and Janetopoulos, 2003; Arrieumerlou and Meyer, 2005; Charest and Firtel, 2006; Levine et al., 2006; Meier-Schellersheim et al., 2006). Although inhibitors are essential components of all gradient sensing models, the spatial-temporal presence of inhibitors has not been examined experimentally.

In this study, we designed sequential stimulation protocols to detect temporal and spatial aspects of the inhibition process in single living cells. We found that repeated transient activations of cAR1 receptor trigger repetitive PH_{Crac}-GFP membrane translocations without detectable refractory periods, demonstrating that a short pulse of cAR1 activation elevates excitation but little long-lasting inhibition. This result provides evidence that cAR1 activation induces an immediate excitation and a delayed recruitment of long-term inhibition leading to PIP_3 accumulation. More significantly, we have revealed spatial distribution of the inhibition process induced by a cAMP gradient. Exposing a cell to a sustained cAMP gradient leads to a stable PH_{Crac}-GFP accumulation in the front of the cell. We found that a sudden withdrawal of the cAMP gradient from this biochemically polarized cell leads to a rapid return of G protein activation, PTEN, and PIP_3 distributions to basal levels around the cell membrane. However, there was a short time period during which reactivation of receptors and G proteins around the membrane induced a clear PIP_3 response in the back but not the front of the cell. This inverted PIP_3 response indicates that a cAMP gradient induces a stronger inhibition of PI3K in the front of a cell.

Results

Brief cAMP stimuli activate excitation but not inhibition of PH_{Crac}-GFP membrane translocation

Previous studies suggest that activation of cAR1 triggers a fast increase of the excitation level and a slower elevation of the inhibition, allowing a cell to respond transiently and then adapt (Iijima et al., 2002; Devreotes and Janetopoulos, 2003; Janetopoulos et al., 2004; Xu et al., 2005). When a sustained cAMP stimulus is removed, cells that had adapted enter a refractory period during which the cells progressively regain their ability to respond to cAMP, suggesting that the inhibition returns to its prestimulus level more slowly than does excitation (Devreotes and Steck, 1979; Dinauer et al., 1980a,b). To test whether there is a temporal difference between the cAR1-induced excitatory and inhibitory processes controlling PIP_3 production, we measured the kinetics of PIP_3 levels around the membrane of cells that were stimulated by multiple transient cAMP stimuli (Fig. 1). We simultaneously visualized and quantitatively measured transiently applied cAMP stimulations and PIP_3 production, reported by the membrane translocation of PH_{Crac}-GFP, a PIP_3 reporter (Parent et al., 1998). Chemotaxis-competent PH_{Crac}-GFP-expressing cells ("PH cells") were treated with Latrunculin B, which eliminates morphological polarity and motility by disrupting the actin cytoskeleton. A micropipette filled with cAMP (1 μM) was placed within 30 μm of PH cells and used in conjunction with a microinjector to deliver a series of brief cAMP stimulations. Alexa 594 was included in the micropipette as a measure of the applied cAMP concentration (Xu et al., 2005). Each cAMP stimulation induced a transient response of PH_{Crac}-GFP membrane translocation (Fig. 1). Temporal changes in cAMP concentration around the cell were determined as the average intensity change of the dye in the R1 and R2 regions (Fig. 1 B). The kinetics of PH_{Crac}-GFP membrane translocation were measured as intensity changes in cytosolic PH_{Crac}-GFP pool (Fig. 1 B), which is inversely related to the amount of membrane-associated PH_{Crac}-GFP (Xu et al., 2005). Quantitative analyses showed that PH_{Crac}-GFP translocation reached its maximal level in 4 s after the cAMP concentration reached its peak, which reflects the temporal delay that is expected for PIP_3 production upon the activation of cAR1 (Fig. 1 C). In our experimental setup, the shortest interval between two transient cAMP stimuli was ∼24 s, a minimal time required for the cAMP concentration to return to its basal level between stimuli (Fig. 1 D). Sequential transient cAMP stimuli with as short as 24-s intervals generated repetitive transient responses of PH_{Crac}-GFP

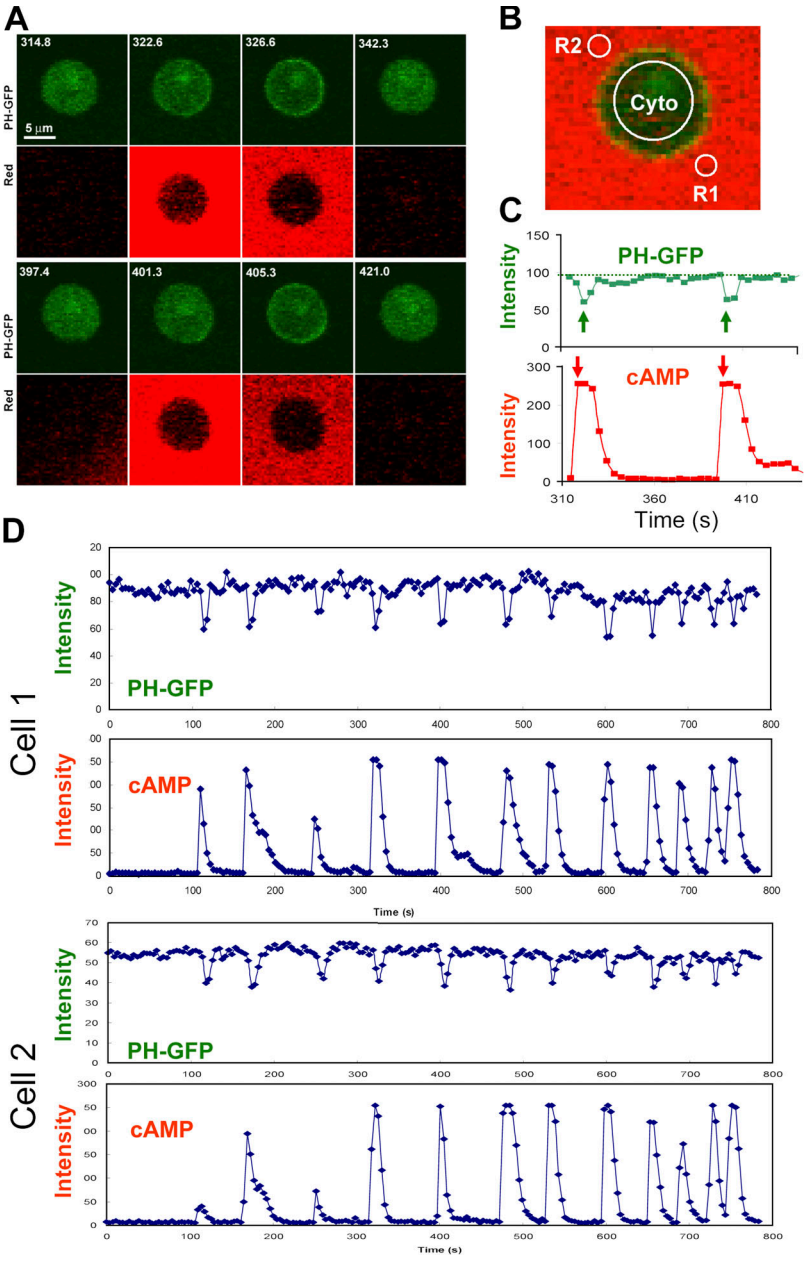

Figure 1. **Transient cAMP stimuli induce repetitive transient PIP_3 responses visualized by the PH_{Crac}-GFP membrane translocation.** (A) Transient cAMP stimulations (red channel) trigger membrane translocations of PH_{Crac}-GFP (green channel) in a living cell. Images were captured at 4-s intervals, and the frames at selected time points are shown here. (B) Temporal changes in cAMP concentration around the cell were measured as the average of fluorescence intensity of Alexa 594 in the regions of R1 and R2. PH_{Crac}-GFP translocation was quantified as the intensity decreases of GFP in the cytoplasm (cyto) of the cell. (C) Dynamic changes in cAMP concentration around the cell (red) and in levels of PH_{Crac}-GFP in cytosol (green) are shown for the selected time period shown in A. (D) Temporal changes in relative levels of PH_{Crac}-GFP in cytosol are shown in the time course for the entire experiment. Temporal changes in the intensity of Alexa 594 were measured in R1 (the front region) and R2 (the back region), which were almost identical in each short pulse under our experimental conditions. Temporal changes in cAMP concentration around the cell are shown as the average fluorescence intensity in R1 and R2 in the time course. The results for two cells are shown.

translocation, and transient responses displayed kinetics without a refractory period (Fig. 1 D). Our data indicate that a transient receptor activation quickly activates excitatory pathways leading to an increase in PIP_3, and upon cAMP removal, these pathways quickly return to prestimulated levels and can be activated again by another cAMP stimulation. Transient cAR1 activations do not signal long enough to substantially elevate the slower inhibition process from its basal level. Therefore, this result supports the idea that cAR1-mediated excitation and inhibition process increases and decreases by following a fast and a slow temporal mode, respectively.

Exposure to cAMP gradient diminishes responsiveness at the front of the cell

The spatial distribution of inhibition in a cell exposed to a cAMP gradient has never been tested. Several models propose that cAR1-induced inhibitors diffuse quickly in a cell, and thus are assumed to be evenly distributed in the inner membrane (Parent and Devreotes, 1999; Iijima et al., 2002; Janetopoulos et al., 2004). However, our dynamic analyses and computer simulations suggest that inhibition mechanisms act locally and predict that inhibition affecting PI3K activity is strongest in the front of a cell at steady state in a cAMP gradient (Xu et al., 2005; Meier-Schellersheim et al., 2006). Because the molecular nature of the inhibitors in chemosensing of *D. discoideum* is still unknown, we developed an approach to indirectly measure the relative extent of inhibition in the front and back of a biochemically polarized cell. We reasoned that after a removal of the cAMP gradient, the signaling network would rapidly return from the polarized to the resting steady state. During this transition, the time required to regain responsiveness to cAMP (the refractory period) may differ between the front and back depending on local

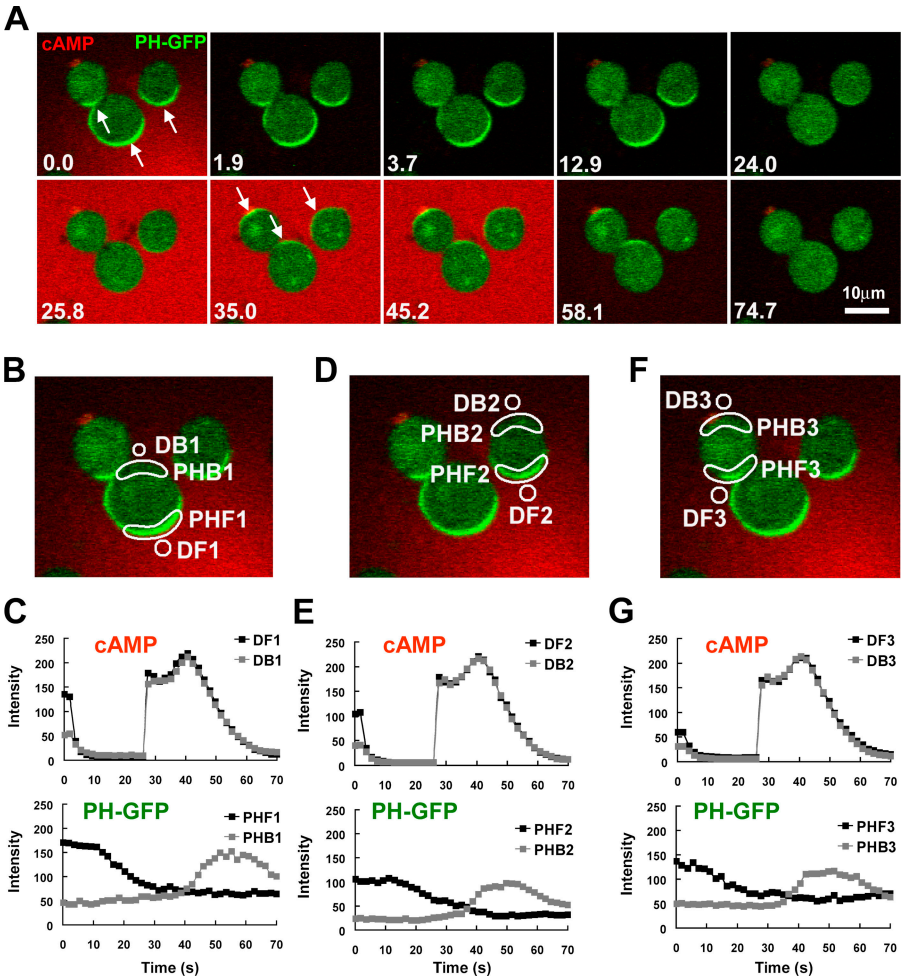

Figure 2. **After a withdrawal of a cAMP gradient from a "polarized" cell, the original front of the cell is temporally less responsive to cAMP stimulation.** (A) Cells expressing PH_{Crac}-GFP (green) were polarized in a cAMP (red) gradient (1 μM cAMP mixed with Alexa594, red) at 0 s (arrows at 0 s point to the fronts). After a withdrawal of the cAMP gradient at 0 s, a uniform cAMP simulation (100 nM of cAMP mixed with Alexa 594) induced PH_{Crac}-GFP translocation to the back (arrows at 35 s) of the cells. An animated version is in the supplemental materials (Video 1, available at http://www.jcb.org/cgi/content/full/jcb.200611096/DC1). Another example is shown as Fig. S1 and Video 2. (B, D, and F). Regions of interest used for assessing concentration changes of cAMP with time in the front (DF1-3) and back (DB1-3), and for quantitative measurement of PH_{Crac}-GFP dynamic changes for the selected front (PHF 1–3) and back (PHB 1–3) membrane regions for each of the three cells shown in A. (C, E, and G) Top panels show temporal changes of Alexa 594 fluorescence for cAMP concentration in the time course in the front (DF) and back (DB) regions. Bottom panels show temporal changes in relative levels of PH_{Crac}-GFP in the front (PHF) and back (PHB) for each of the three cells.

concentrations of inhibitors induced by the prior gradient. In our experiments (Fig. 2), PH cells were first exposed to a cAMP gradient until they achieved a stably polarized state, in which PH_{Crac}-GFP accumulated in the front. After quickly withdrawing the gradient at time 0, we observed that PH_{Crac}-GFP rapidly returned to the cytosol. Before the cells could fully return to the resting state, which may take ~6 min (Devreotes and Steck, 1979; Devreotes, 1994), they were challenged with a uniformly applied cAMP stimulus. Interestingly, this induced an "inverted" response in which PH_{Crac}-GFP transiently translocated to the back of the cells, demonstrating that the original front sides of the cells were less responsive to cAMP than were the back sides. Moreover, cells that had been exposed to gradients of various cAMP concentrations for the initial stimulus also exhibited inverted PH_{Crac}-GFP responses upon a uniform cAMP stimulation (Fig. 2, B–G; and Fig. S1, available at http://www.jcb.org/cgi/content/full/jcb.200611096/DC1).

After the removal of a cAMP stimulus, G proteins quickly reassociate and can be reactivated

The observed inverted PIP_3 response is likely caused by a slow return of the intracellular components to their "resting" states because the average time period for cAMP binding to the receptor is in the range of seconds (Ueda et al., 2001). Several components in the pathways may be responsible for the differential refractory behaviors of the front and back of the cells. For example, receptors may remain asymmetrically desensitized or G proteins may not be completely reassociated upon the second cAMP stimulation. We addressed this issue by directly measuring the kinetics of G protein reassociation and reactivation in living cells using FRET analysis (Fig. 3). Cells expressing Gα2-CFP and YFP-Gβ ("G cells") were suddenly exposed to 10 μM cAMP (Fig. 3, A and B), a saturating dose for cAR1, or 1 μM cAMP (Fig. S2, available at http://www.jcb.org/cgi/content/full/jcb.200611096/DC1). Addition of cAMP induced a rapid FRET loss, which reached a steady state in <20 s, indicating G protein dissociation (Fig. 3 B; Fig. S2) (Xu et al., 2005). After the removal of cAMP, FRET returned to the prestimulus level in ~60 s, indicating that the G proteins were completely reassociated. A second sudden exposure to the same concentration of cAMP triggered an instant FRET loss that displayed kinetics very similar to those in response to the first stimulation (Fig. 3 B; Fig. S2), demonstrating that cAR1 receptor and G proteins rapidly returned to their prestimulation states and could be fully reactivated within 60 s after the removal of cAMP.

We then simultaneously monitored temporal changes in the receptor/G protein activation and PH_{Crac}-GFP translocation in the front and back of the cells previously exposed to a cAMP gradient (Fig. 3, C–F). We measured FRET changes in one G cell

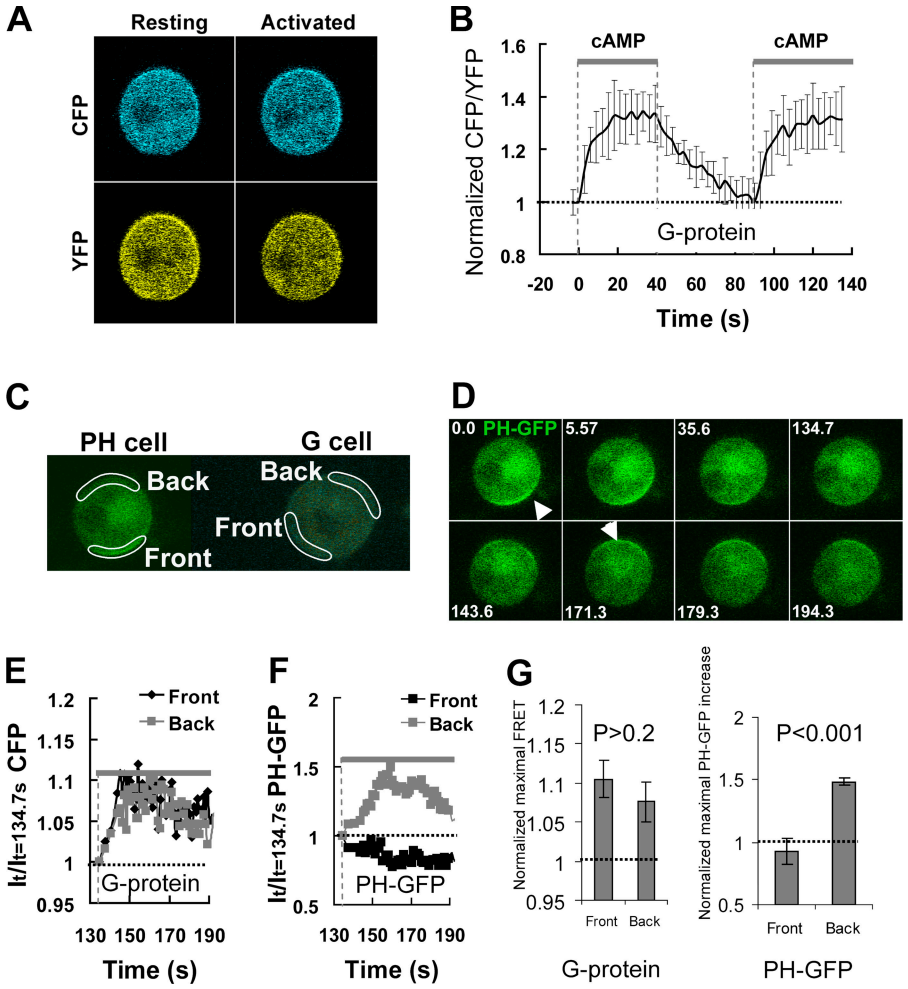

Figure 3. **Single-cell FRET measurement of kinetics of G protein dissociation (activation), association (inactivation) and redissociation (reactivation), and temporal relationship between G protein reactivation and the inverted PH_{Crac}-GFP translocation.** (A) Cells expressing Gα2-CFP and YFP-Gβ (G cells) were suddenly exposed to cAMP field (10 μM) at 0 s. The cAMP field was suddenly removed at 42 s and reapplied at 93 s. Fluorescence images of CFP and YFP of a G cell at resting or fully activated stages. (B) Temporal changes in G protein activation at the cell membrane. A normalized FRET change (expressed as CFP/YFP ratio) indicates relative level of G protein activation at the cell membrane. Kinetics of cAMP mediated changes in the FRET ratio in the entire membrane of single G cells are shown as means ± SD ($n = 7$). The thick gray bars show temporal changes in cAMP concentration. The thin black dashed line shows the basal level of FRET, which is 1. (C) The spatiotemporal relationship of G protein activation and the inverted PH_{Crac}-GFP response. cAMP-mediated G protein activation was measured in the front and back regions of a G cell, and cAMP-induced PIP_3 changes were monitored by PH_{Crac}-GFP dynamics in the front and back of a nearby (within 20 μm) PH cell. A cAMP gradient (1 μM cAMP released from a micropipette) was suddenly withdrawn from the G and PH cells at 0 s. A uniform cAMP field (100 nM), applied at 134 s, induces a clear PH_{Crac}-GFP translocation to the back of the PH cell. An animated version is in Video 2 (available at http://www.jcb.org/cgi/content/full/jcb.200611096/DC1). Regions of interest for simultaneous measurement of G protein activation in one G cell and the inverted PIP_3 response in a PH cell are shown. (D) Selected images show the inverted PH_{Crac}-GFP translocation in the experiment shown in C. The arrows point to direction of PH_{Crac}-GFP membrane translocation: the original at 0 s and the inverted at 171 s. (E) The temporal changes in the G protein dissociation in the front (black) and back (gray) of the G cell, reflected as CFP intensity changes, in response to the uniform cAMP field. The basal level of G protein activation is 1, shown as the thin line. The thick gray bar indicates the temporal changes in cAMP concentration. (F) Temporal changes in PH_{Crac}-GFP in the front and back of the PH cell in response to the uniform cAMP stimulation applied at 134 s. The basal levels of PH_{Crac}-GFP in the front and back are 1, indicated as the thin dashed line. The thick gray bar indicates the temporal changes in cAMP concentration. (G) After a withdrawal of a gradient, a new uniformly applied cAMP field induced similar levels of G protein dissociation in the front and back of G cells, but triggered a clear PH_{Crac}-GFP translocation only to the back regions of PH cells. Normalized maximal FRET changes and PH_{Crac}-GFP increases in the front and back of G and PH cells are shown as means ± SD ($n = 5$). Basal levels are 1, indicated as dashed line.

and PH_{Crac}-GFP translocation in another PH cell. The cells were located within 20 μm and thus both were exposed to very similar cAMP stimuli (Fig. 3 C). After a rapid withdrawal of a cAMP gradient at time 0, the G protein reassociated around the G cell membrane and PH_{Crac}-GFP returned to the cytosol (Fig. 3 D). A uniformly applied stimulation at 134.7 s triggered a similar degree of G protein dissociation, which was measured as a CFP fluorescence increase (FRET loss), in both the front and back of the G cell (Fig. 3 E), while a distinctive accumulation of PH_{Crac}-GFP only occurred in the back of the PH cell (Fig. 3, D and E). Because the subsequent cAMP stimulation induced G protein activation in both the front and back, we concluded that the possible asymmetrical desensitization of cAR1 receptors, such as cAR1 phosphorylation induced by the first cAMP gradient, could not explain the subsequent PH_{Crac}-GFP translocation only to the back of the cell (Fig. 3 G). Thus, the inverted PIP_3 response is likely caused by inhibitory mechanisms acting on the signaling components downstream of cAR1 and the heterotrimeric G proteins.

Spatiotemporal dynamics of PH_{Crac}-GFP membrane translocation in PTEN null cells in response to cAMP stimuli

cAR1 activates an excitatory signaling branch that induces PTEN to translocate from the membrane to the cytosol and also elevates an inhibitory mechanism that allows cytosolic PTEN to return to the membrane (Funamoto et al., 2002; Iijima and Devreotes, 2002). To determine spatiotemporal changes in PIP_3 in the cells lacking PTEN, we measured kinetics of PH_{Crac}-GFP membrane translocation in *pten*$^-$ cells and compared the kinetics to those in wild-type (WT) cells (Xu et al., 2005; Meier-Schellersheim et al. 2006), in response to uniformly applied cAMP and a cAMP gradient (Fig. 4). WT and *pten*$^-$ cells expressing PH_{Crac}-GFP were stimulated uniformly with cAMP (1 μM) at 0 s (Fig. 4 A). The cAMP-triggered PH_{Crac}-GFP membrane translocation is fast and transient in WT cells. In contrast, the response in *pten*$^-$ cells was clearly slower, peaking in ∼12 s and returning to prestimulus levels in more than 40 s (Fig. 4 A).

When the cells were suddenly exposed to a gradient (Fig. 4 B), membrane translocations of PH_{Crac}-GFP occurred initially in both front and back regions in both WT and *pten*$^-$ cells. However, the kinetics of PH_{Crac}-GFP translocation in the front was clearly abnormal in *pten*$^-$ cells. There was no clear decrease in PH_{Crac}-GFP amount at the front for more than 150 s, which differs from the biphasic response in WT cells (Fig. 4 B). We also examined kinetics of the PIP_3 in response to the removal of cAMP stimuli in *pten*$^-$ cells (Fig. 4 C). After cells were exposed to a gradient, PH_{Crac}-GFP accumulates in the front regions of WT or *pten*$^-$ cells. Upon a removal of the gradient at 0 s, PH_{Crac}-GFP gradually returned to the cytosol. The returning process was clearly slower in *pten*$^-$ cells than in the WT cells, whose $t_{1/2}$ were ~22 s and 14 s, respectively (Fig. 4 C).

PTEN quickly redistributes to the membrane after cAMP removal

PTEN is involved in regulating spatiotemporal dynamics of PIP_3 levels around the membrane of a cell in response to cAMP stimulation. Therefore, the dynamic distribution of PTEN affects the local PIP_3 levels. When a cell reaches the "polarized" steady state in a stable cAMP gradient, PTEN is enriched at the back side of a cell (Funamoto et al., 2002; Iijima and Devreotes, 2002; Li et al., 2005). After withdrawal of the cAMP gradient, PTEN starts to redistribute itself from the polarized to the resting steady state. During this transition, a transient accumulation of PTEN in the front could potentially explain the inverted PIP_3 response. To address this possibility, we measured the spatiotemporal dynamics of PTEN under these conditions (Fig. 5). After a rapid withdrawal of the gradient at time 0 (Fig. 5, A and B), PTEN redistributed from the back and became uniformly distributed around the membrane in ~80 s without over-accumulating in the front (Fig. 5). Furthermore, reapplying a uniform stimulus (Fig. 5, A–D) or gradient (Fig. 5, E–H) of cAMP induces PTEN translocation with kinetics (Fig. 5) similar to those observed in the cells that had not previously been stimulated (Meier-Schellersheim et al., 2006), indicating that the cAR1-controlled regulatory components of PTEN returned to their "resting" states and PTEN molecules in both the front and back were responsive to a second cAMP stimulation when the inverted PH_{Crac}-GPF response occurred. Therefore, the excitatory and the inhibitory mechanisms that control PTEN membrane distribution are not the likely explanation for this inverted response.

Inhibitory pathways controlled by Gα1 or Gα9 subunits are not essential for cAR1-mediated PH_{Crac}-GFP responses

Other mechanisms may also be involved in inhibition in the signaling network of cAMP gradient sensing. For example, Gα9 and Gα1-mediated PLC pathways in *D. discoideum* have been shown to function as negative regulators in the cAR1-mediated signaling (Bominaar and Van Haastert, 1993; Brzostowski et al., 2004). To test whether either pathway is essential for the gradient sensing, we examined PH_{Crac}-GFP responses in Gα9 and Gα1 null cells (Fig. 6). We measured PH_{Crac}-GFP membrane translocation by monitoring intensity changes of GFP fluorescence

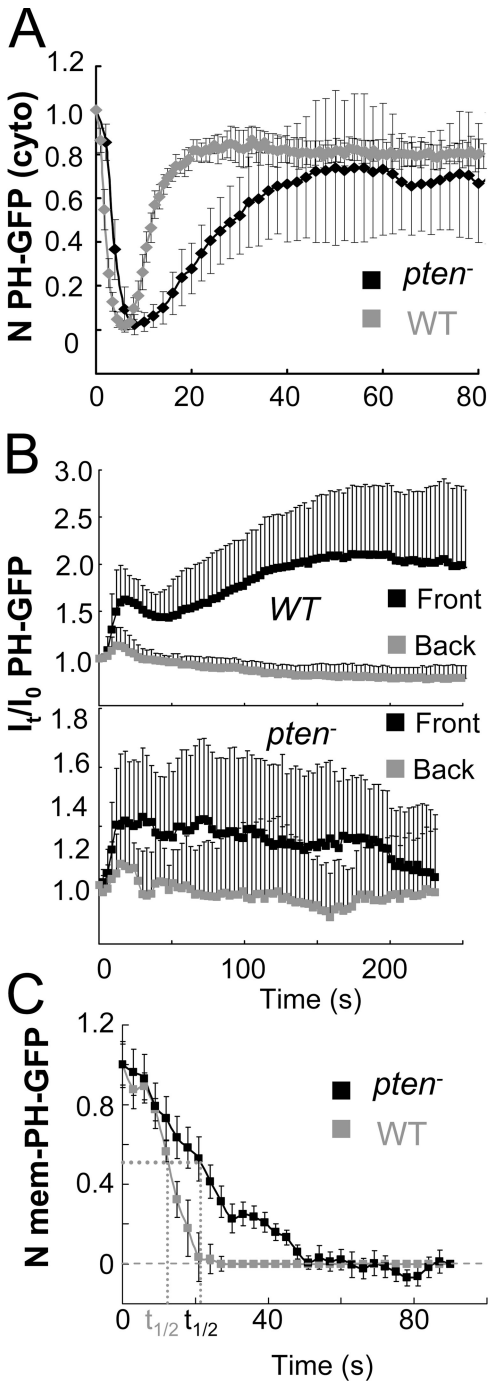

Figure 4. **Dynamics of PH_{Crac}-GFP membrane translocation in PTEN null cells upon a uniform and a gradient of cAMP stimulations.** (A) WT and *pten*$^-$ cells expressing PH_{Crac}-GFP were uniformly stimulated with cAMP (1 μM). Kinetics of PH_{Crac}-GFP membrane translocation are shown as the normalized intensity changes in cytosolic PH_{Crac}-GFP, where the intensity at time 0 is defined as 1 and the minimal intensity is defined as 0. (B) WT (top panel, as a control) and *pten*$^-$ cells expressing PH_{Crac}-GFP were suddenly exposed to a cAMP gradient. Temporal changes in relative levels of PH_{Crac}-GFP in the front and back of the cells. Means ± SD (n = 8) are shown. (C) Kinetics of membrane-bound PH_{Crac}-GFP in the front of WT, as a control, and *pten*$^-$ cells in response to a withdrawal of an applied cAMP stimulation. Means ± SD (n = 10) are shown.

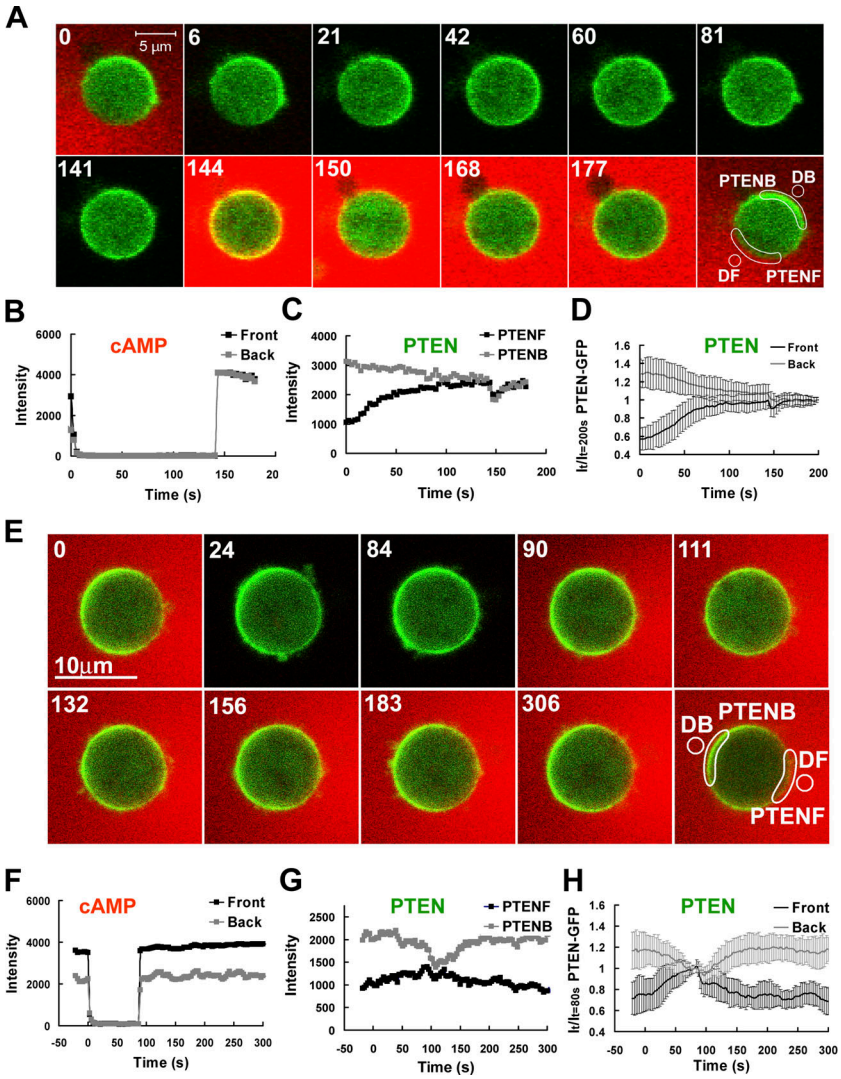

Figure 5. **Spatiotemporal dynamics of PTEN in single cells upon a withdrawal of a cAMP gradient and then stimulated with a uniform dose (A–D) or a gradient (E–H) of cAMP.** (A). A PTEN-GFP expressing cell was highly polarized in a stable cAMP gradient (red, 1 μM in the micropipette, red) at 0 s. The gradient was suddenly withdrawn from the cell at 0 s. A uniform cAMP stimulation (100 nM) was applied at 144 s. Regions of interest for the data reported in B and C are also shown. (B) Temporal changes in cAMP concentrations in the front (black) and back (gray) are shown in the time course. (C) Temporal changes in relative levels of membrane-bound PTEN in the front (black) and back (gray) regions are shown in the time course. (D) Kinetics of membrane-bound PTEN in the front and back are shown as means ± SD (n = 10) in response to a withdrawal and then to a uniformly applied stimulation. (E) A PTEN-GFP expressing cell was highly polarized in a stable cAMP gradient (red, 1 μM in the micropipette) at 0 s. The gradient was suddenly withdrawn from the cell start at 0 s, and reapplied at the 90 s. Regions of interest for the data reported in B and C are also shown. Animated version is in the supplemental materials (Video 4, available at http://www.jcb.org/cgi/content/full/jcb.200611096/DC1). (F) Temporal changes in cAMP concentrations in the front (black) and back (gray) are shown in the time course. (G) Temporal changes in relative levels of membrane-bound PTEN in the front (black) and back (gray) regions are shown in the time course. (H) Kinetics of membrane-bound PTEN in the front and back are shown as means ± SD (n = 13) in response to a withdrawal and reapplied of the cAMP gradient.

in the cell membrane (Xu et al., 2005). In response to a uniform stimulation, the spatiotemporal kinetics of PH_{Crac}-GFP membrane translocation in either gα9$^-$ or gα1$^-$ were similar to those in the WT cells (Fig. 6, A and C). When the gα9$^-$ or gα1$^-$ cells were suddenly exposed to stable cAMP gradients, PH_{Crac}-GFP translocation, as in WT cells, consisted of two phases, an initial transient translocation around the cell membrane followed by a second phase producing a highly polarized distribution (Fig. 6, B and D). Because our observed dynamics in both mutant cells are similar to those displayed in WT cells (Xu et al., 2005; Meier-Schellersheim et al. 2006), we suggest that Gα1 or Gα9 controlled signaling are not essential inhibitory mechanisms for cAR1-mediated gradient sensing.

Local inhibition mechanism of PI3K revealed by a cAMP-gradient-induced inverted PH_{Crac}-GFP translocation

We speculated that the inverted PH_{Crac}-GFP translocation may be induced by a reapplied cAMP gradient. Fig. 7 shows this experiment. A WT cell expressing PH_{Crac}-GFP was first equilibrated in a cAMP gradient to achieve the polarized state. After a withdrawal of the cAMP gradient at time 0 s, PH_{Crac}-GFP returned to cytosol. At 81 s, the identical gradient was reapplied (Fig. 7, A and B). In response to this second gradient, the cells exhibited a much stronger transient accumulation of PH_{Crac}-GFP in the back than in the front (Fig. 7, A and B). Fig. 7 C shows the comparison of normalized increase in cAMP concentration delivered by the second gradient in the front and back regions of the cells; and Fig. 7 D shows the maximal increase in PH_{Crac}-GFP in the front and back regions during the inverted responses (n = 8). Our results show that, despite the cAMP stimulus being higher in the front than in the back, the cells responded only in the back regions. Thus, after a withdrawal of the gradient, the cells displayed an asymmetrical refractory period. During this period, PIP_3 initially accumulated in an intracellular gradient that had the opposite direction of the external cAMP gradient. The asymmetrical refractory period could be detected in some cells for more than four minutes after the withdrawal of the previous gradient (Fig. S3, available at http://www.jcb.org/cgi/content/full/jcb.200611096/DC1).

It was previously reported that cAMP receptor-mediated PI3K activation consists of two layers in chemotaxing cells. First, free Gβγ activates Ras that stimulates a small amount of preexisting, membrane-associated PI3K. The resulting actin

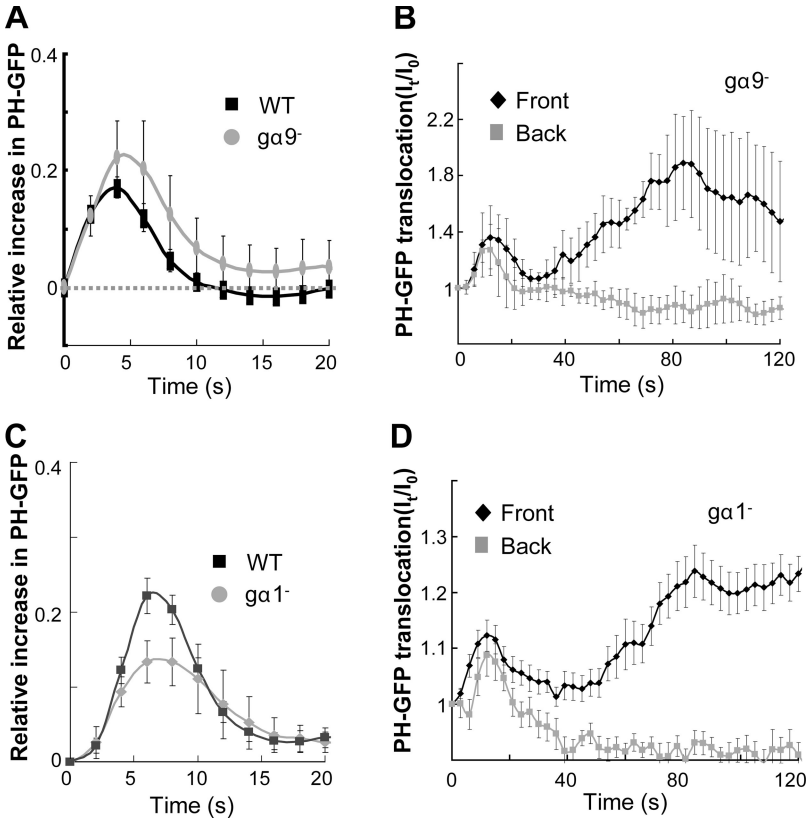

Figure 6. **Gradient sensing appears normal in the cells lacking Gα9 and Gα1 subunits.** (A and B) Gα9 null cells expressing PH_{Crac}-GFP were stimulated by a uniformly applied cAMP (A) or by a cAMP gradient (B, and Fig. S4 A). (C and D) Gα1 null cells expressing PH_{Crac}-GFP were stimulated by a uniformly applied cAMP (C) or by a cAMP gradient (D). Stimulations were applied at time 0. Temporal changes in relative levels of PH_{Crac}-GFP in the membrane are shown in the time course.

polymerization leads to recruitment of additional PI3K from cytosol to the membrane, thereby increasing the amount of active PI3K (Sasaki et al., 2004). In Latrunculin-treated cells, PI3Ks were uniformly distributed around the membrane of the cells even when they were exposed to the cAMP gradient (Sasaki et al., 2004; unpublished data). Therefore, under our experimental condition, we monitored the spatiotemporal regulations of PI3K activity without complications from the second layer of actin-dependent PI3K recruitment. In addition to the signaling pathway leading to PI3K activation, the cAMP receptor also regulates another pathway mediating the redistribution of membrane-bound PTEN, which is important for the proper directional response of PIP_3. In *pten*$^-$ cells, PH_{Crac}-GFP was still able to accumulate in the front when the cells were exposed to a cAMP gradient (Janetopoulos et al., 2004; Sasaki et al., 2004). We found that the crescents of PH_{Crac}-GFP in *pten*$^-$ cells were broader than those formed in WT cells (Fig. 7, E and F; at time 0), as previously described (Janetopoulos et al., 2004; Sasaki et al., 2004). Furthermore, the directions of the crescents, unlike those in WT cells, did not always perfectly point to the direction of the gradient (Fig. 7 F; at time 0). These results indicate, as expected, that a cAMP gradient-induced PTEN redistribution ensures the PIP_3 response in the restricted front region, and this directional response was not precise without PTEN. However, after a withdrawal of the cAMP gradient, PH_{Crac}-GFP returned to cytosol. More importantly, the second cAMP gradient induced the inverted PH_{Crac}-GFP membrane translocation in *pten*$^-$ cells (Fig. 7, E and F), indicating that a cAMP gradient-induced asymmetrical inhibition occurred in the absent of PTEN. Collectively, our results suggest that the previous gradient induced an asymmetrically distributed and locally controlled inhibition and this localized inhibition acts on the signaling pathway between free Gβγ to PI3K.

Kinetics of the asymmetrical inhibition induced by a cAMP gradient

We examined the temporal appearance and disappearance of the gradient-induced asymmetrical inhibition (Fig. 8; Fig. S4, B and C, available at http://www.jcb.org/cgi/content/full/jcb.200611096/DC1). We found that a brief gradient stimulation of ∼50 s was not sufficient to induce an inverted PH_{Crac}-GFP response (Fig. 8, A and B; Fig. S4 B). Thus, exposure to a stable gradient for ∼2 min is needed to establish an asymmetrical inhibition. Furthermore, cells that were removed from a gradient for 6 min and rechallenged with either uniform cAMP stimulation or a cAMP gradient displayed a noninverted PH_{Crac}-GFP translocation response as in naive cells (Fig. 8, C and D; Fig. S4 C), indicating that asymmetrical inhibition disappears within 6 min after the gradient is removed.

Discussion

The existence of inhibitory components in GPCR-mediated chemosensing has been proposed for more than thirty years, but the molecular mechanisms are still unknown and, thus, cannot yet be visualized directly. Here, we report insights into the temporal and spatial aspects of the inhibition based on measurements of the spatiotemporal dynamics of known components of the gradient sensing machinery aided by our computational modeling study.

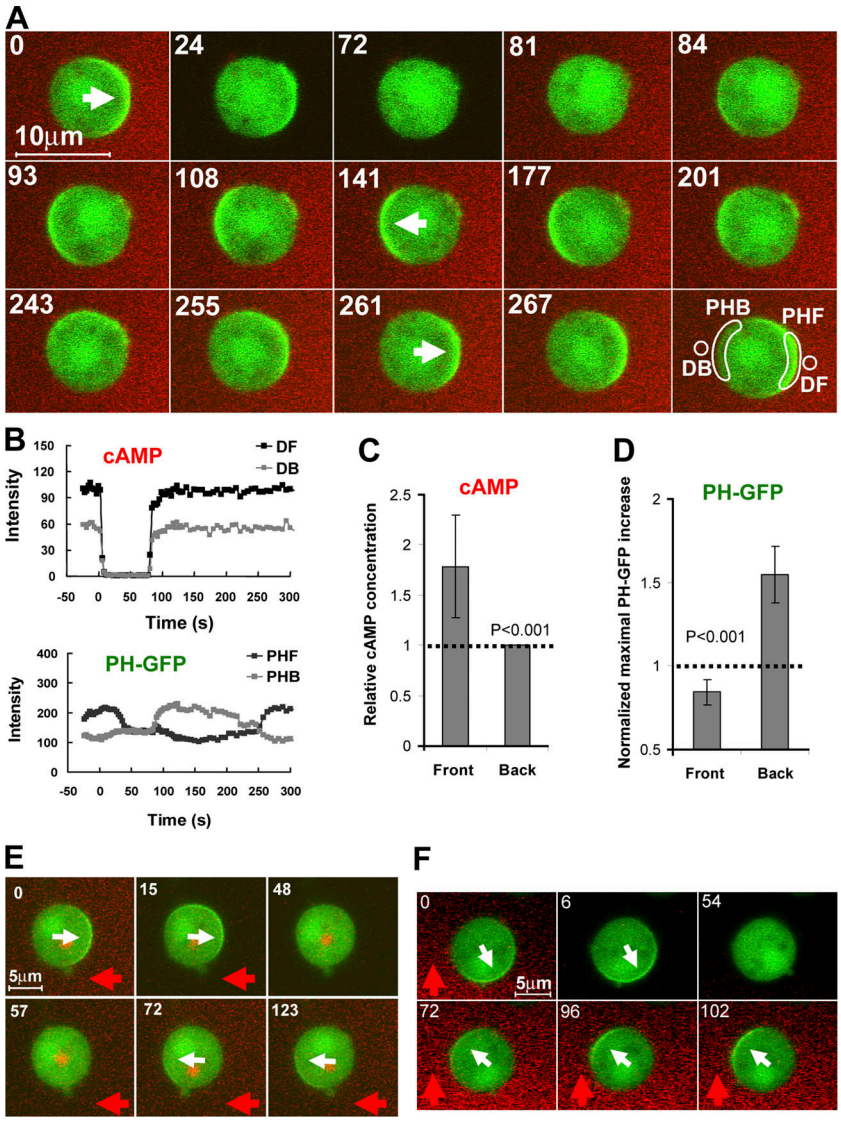

Figure 7. **An inverted PH_{Crac}-GFP translocation can be induced by a reapplied cAMP gradient.** (A) In a stable cAMP gradient, PH_{Crac}-GFP enriched in the front of a WT cell at 0 s. Upon the withdrawal of the cAMP gradient at 0 s, PH_{Crac}-GFP gradually returned to the cytosol. At 81 s, the same gradient was reapplied around the cell, PH_{Crac}-GFP initially translocated to the back side of the cell and formed a clear crescent from 93 s to 177 s. From 201 s, the PH_{Crac}-GFP crescent started to turn toward the front, and the crescent eventually localized in the front of the cell. Images were captured at 2-s intervals, and the frames at selected time points are shown. Regions of interest used to assess concentration changes in cAMP and dynamics of PH_{Crac}-GFP in the front and back of a cell are shown. Video 5 shows a full set of images from one experiment (available at http://www.jcb.org/cgi/content/full/jcb.200611096/DC1). Another example is shown as Fig. S2 and Video 6. Regions of interest used to assess concentration changes in cAMP and PH_{Crac}-GFP are shown. Front (DF) and back (DB) regions used to evaluate quantitative changes of Alexa 594 as a measure of cAMP concentration. PHF and PHB were selected membrane regions used for monitoring the responses of PH_{Crac}-GFP translocation to the front and back of the cell, respectively. (B) Temporal changes in cAMP concentrations (top panel) and in PH_{Crac}-GFP (bottom panel) in the front (black) and the back (gray) regions of the cell. (C) After a withdrawal of gradients, new gradients were applied to the PH cells that were in the transients from polarized stages to resting stages. The fronts of the cells were exposed to higher concentrations of cAMP, comparing DF to DB (cAMP concentration in the back). Means ± SD are shown (n = 8). (D) PH_{Crac}-GFP initially translocated only to the back of the cells, comparing PH-B to PH-F. Maximal PH_{Crac}-GFP translocation responses are shown as means ± SD (n = 8). The basal levels are 1, indicated as the thin dashed line. (E and F) In *pten*$^-$ cells, the inverted PH_{Crac}-GFP translocations were induced by a reapplied cAMP stimulation. The white arrows indicate the direction of PH_{Crac}-GFP accumulation. The red arrows indicate the directions of cAMP gradients. Images were captured at 3-s intervals, and the frames at selected time points are shown.

We have constructed a quantitative model for cAR1-mediated signaling network (Meier-Schellersheim et al., 2006). The model, which includes receptor-mediated and locally controlled inhibitory mechanisms that regulate PI3K and PTEN (Fig. 9 B), simulates experimentally determined dynamics of receptor activation, G protein dissociation, PTEN membrane localization, and PIP_3 accumulation (Meier-Schellersheim et al., 2006). For example, in response to a uniform cAMP stimulus, the model generates a transient PIP_3 response that quickly returns to the resting stage (adaptation). When exposed to a cAMP gradient, a cell generates a steeper PIP_3 gradient by initially inducing a PIP_3 increase followed by a PIP_3 decrease around the membrane, and then producing a highly polarized distribution of PIP_3 in 120 s (amplification) (Fig. S5, available at http://www.jcb.org/cgi/content/full/jcb.200611096/DC1). During the amplification process, the membrane-bound PTEN gradually translocates from the front to the back, while the amount of the membrane-associated PI3K remains the same around the membrane (Fig. 9 C). Temporal changes in PI3K activity in the front and back, which cannot be directly visualized, have been simulated by the model based on dynamics of PIP_3 and membrane-bound PTEN (Meier-Schellersheim et al., 2006; Fig. S5). Previous study and our measurements indicated that when a cell reaches the "polarized" steady state, the amount of PI3K in the front is almost equal to that in the back (Sasaki et al., 2004). PIP_3 is at a higher steady-state level in the front. However, this level does not continue to increase ($\Delta PIP_3/\Delta t = 0$) in spite of a lower level of PTEN. At the same time, in the back, a higher level of PTEN does not result in a continuous decrease in the PIP_3 level ($\Delta PIP_3/\Delta t = 0$). Two possible models may explain different steady states of PIP_3 in a polarized cell. First, PI3K activity is stronger than that of PTEN in the front, and PIP_3s are continually produced. The PIP_3 level remains steady in the front because it diffuses fast enough to be degraded by PTEN that is enriched in the back, which is expected from models containing only globe inhibition mechanisms (Parent and Devreotes, 1999; Iglesias and Levchenko, 2002; Iijima et al., 2002). Second, balances between the activities of PI3K and PTEN have been reached in both the front and back, and the balances are achieved by a stronger inhibition of PI3K activity in the front, which

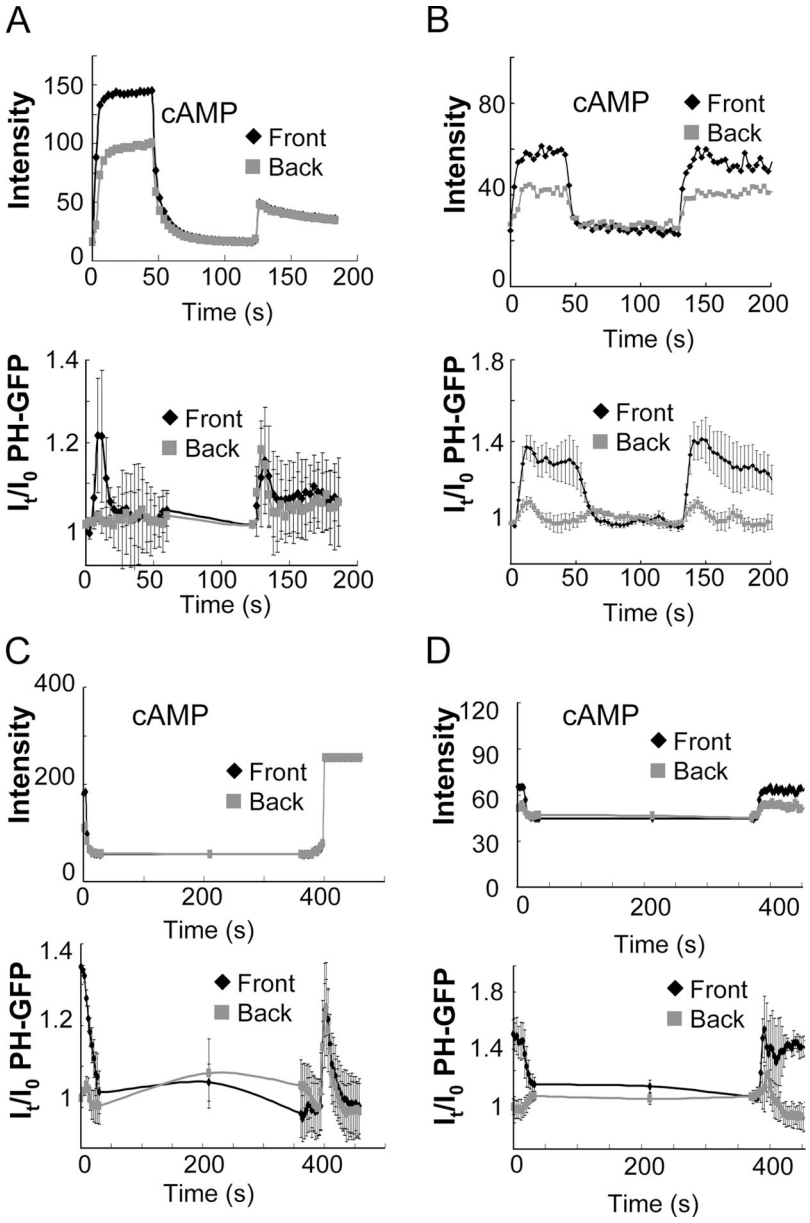

Figure 8. **Kinetics of the asymmetrically distributed inhibition.** (A and B) Asymmetrically distributed inhibition is not induced by exposure to an initial cAMP gradient for just 50 s. PH cells were suddenly exposed to a cAMP gradient (1 μM) at 0 s for 50 s. After a withdrawal of the gradient for ~70 s, a uniform cAMP stimulation (100 nM) induced PH_{Crac}-GFP translocation in both the original front and the back regions (A); and a reapplied cAMP gradient triggered a clear PH_{Crac}-GFP translocation in the original front (B). (C and D) The asymmetrical inhibition disappears 6 min after the removal of the cAMP gradient. PH cells had been exposed to a cAMP gradient (1 μM) for more than two min, and PH_{Crac}-GFP became stably polarized in the front of the cells. The cAMP gradient was removed from the cells at 0s. After a removal of the gradient for 6 min, a uniform cAMP stimulation (100 nM) induced a PH_{Crac}-GFP translocation in both the original front and the back regions (C), and a reapplied cAMP gradient triggered PH_{Crac}-GFP translocations to both the original front and back regions.

have been proposed in our model that includes local inhibition mechanisms (Xu et al., 2005; Meier-Schellersheim et al., 2006). Because different proposed mechanisms could lead to high chemotactic sensitivity in theory (Meinhardt, 1999; Postma and Van Haastert, 2001; Devreotes and Janetopoulos, 2003; Arrieumerlou and Meyer, 2005; Levine et al., 2006; Meier-Schellersheim et al., 2006), we designed experiments to determine which inhibitory mechanisms are likely used in GPCR-mediated chemosensing. In this study, we revealed spatiotemporal features of an inhibitory process that acts locally on the activation pathway between Gβγ and PI3K.

There is a general agreement that inhibition increases and decrease slowly in response to the changes of cAMP receptor occupancy (Parent and Devreotes, 1999; Iglesias and Levchenko, 2002; Iijima et al., 2002; Meier-Schellersheim et al., 2006). Several lines of evidence are consistence with this notion. We showed that a series of cAMP short pulses induce multiple transient PIP_3 responses without detectable refractory periods, suggesting that a quick increase and decrease of cAR1 receptor occupancy immediately turns on and off the excitation process leading to PIP_3 production but does not significantly elevate the slower inhibition process (Fig. 1). We previously reported that a sustained cAMP stimulation induces persistent G protein dissociation while the PIP_3 increases transiently, returning to basal levels within a minute (Xu et al., 2005). Thus, the inhibition that is responsible for the adaptation is most likely caused by an increase in the level of negative regulators controlling the signaling components other than cAR1 and G proteins around the membrane. When a cAMP stimulation was rapidly removed from an adapted cell, the G proteins reassociated and PTEN returned to its prestimulus, membrane-associated state in about one minute and could be fully reactivated by another cAMP stimulation (Fig. 3, and Fig. 5). When a cAMP gradient was removed from a polarized cell, there was a short

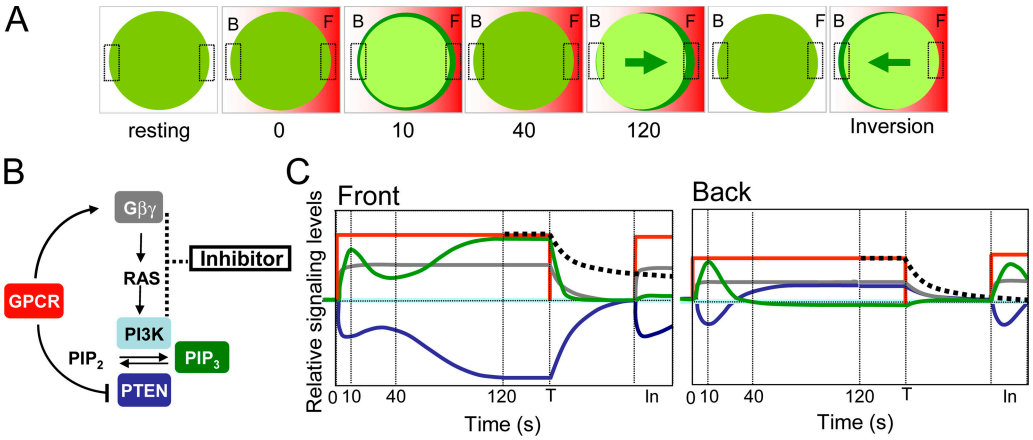

Figure 9. **Dynamic signaling events in a cell exposed to a gradient of cAMP leading to PIP_3 polarization, followed by a withdrawal of the gradient and then reapplying the gradient inducing an inverted PIP_3 response.** (A) A cell is shown schematically at several time points, indicating the distributions of extracellular cAMP (red) and intracellular PH_{Crac}-GFP (green) in the front (F) and back (B) regions. (B) A scheme of GPCR-mediated signaling network containing inhibitory mechanisms. Dynamics of signaling molecules that are filled with colors were measured in living cells. Activation of GPCR: cAMP (red), G protein dissociation, free Gβγ (gray), membrane-bound PTEN (blue), membrane-bound PI3K (light blue), PIP_3 levels (green), and inhibitory components (black box). (C) Graphs represent a time course of relative signaling levels in the front and back of a cell. A naive cell at resting stage is suddenly exposed to a stable cAMP gradient at time 0. The cell reaches a polarized steady-state at 120 s. At the time T, the cAMP gradient is quickly removed, the cell starts to return to its resting stage. Before the cell completely returns to the resting stage, the cAMP gradient is reapplied, and the cell generates an inverted PIP_3 response at time "In". During this time course, the relative levels of extracellular cAMP (red), the extent of G protein dissociation (gray), membrane-associated PH_{Crac}-GFP (green) as a measure of PIP_3 levels, membrane-associated PTEN (blue), the amount of membrane-associated PI3K (light blue, the PI3K activity has not been directly measured. Temporal changes in PI3K activity was simulated, shown in Fig. S5), and the proposed inhibition (black dash lines) in the front and back of the cell are shown.

period of time during which another cAMP stimulation triggers G protein dissociation and PTEN translocation in both the front and back but induces PIP_3 responses only in the back of the cell (Fig. 9). This suggests that inhibitors that are more abundant in the front block transmission of activating signals from Gβγ to PI3K (Fig. 9, B and C). The relatively slower recovery of the responsiveness in PIP_3 production in the front of the cell revealed that the inhibitory effect diminished slowly. The fact that the PH_{Crac}-GFP inversion response was also observed in *pten*$^-$ cells indicated that the recruitment of inhibitors does not depend on PTEN (Fig. 7, E and F). Postma et al. (2004) reported that cells that were stimulated with a sustained uniform cAMP field did not result in a clear decrease in PIP_3 production to another cAMP stimulation, suggesting that the recovery period is very short in a cell that has adapted to a uniform cAMP concentration. It is possible that a high level of the inhibitor is only induced by a cAMP gradient at the front of a cell where the PIP_3 level is high but not by a uniform cAMP around the cell membrane where the PIP_3 level remains low. We can only speculate on this point before the putative inhibitors in GPCR-mediated chemosensing network are identified.

The inhibition has been assumed to be "global" or uniformly distributed throughout the plasma membrane even when a cell is exposed to a cAMP gradient (Parent and Devreotes, 1999; Iglesias and Levchenko, 2002; Iijima et al., 2002; Devreotes and Janetopoulos, 2003; Janetopoulos et al., 2004). Our findings demonstrate that the concept of a purely global inhibition cannot be reconciled with the observed spatial distributions of some inhibitory mechanisms. The inverted PIP_3 response upon restimulation indicates that a sustained cAMP gradient induces an asymmetrically distributed inhibition that acts on the signaling pathway between G protein and PI3K (Fig. 7). This inhibition is stronger in the front of the cell. The spatiotemporal features of the inhibition can shed light on unknown molecular mechanisms. Based on the fast-diffusive-inhibition models, small molecules, such as Ca^{2+} or cGMP, were suggested to be candidate inhibitors, which have not been verified by experiments. The "local excitation and global inhibition" model assumes the presence of a negative regulator, and suggests that it is likely to be PTEN. Based on our detailed spatiotemporal dynamics of PTEN and PIP_3, our computational model showed that PTEN alone cannot fully explain the experimentally determined dynamics (Meier-Schellersheim et al., 2006). We proposed, in addition to PTEN, other inhibitory mechanisms that may involve reversible modifications of components in the pathway from free Gβγ to Ras and then to PI3K. Previous studies in mammalian GPCR signaling indicated several inhibitory components. After GPCR activation, free Gβγ dimers interact with the receptor-associated kinase GRK2, blocking Gβγ signaling (Lodowski et al., 2003). GPCR activation can also induce a translocation of a RasGAP, which binds to PIP_3, to inner membrane deactivating Ras thereby inhibiting PI3K (Lockyer et al., 1999). In *D. discoideum*, it has been shown that a sustained cAR1 activation, which triggers a persistent G protein dissociation, induces a transient activation of RasG, which activates PI3K (Sasaki et al., 2004). The transient nature of RasG activation is consistent with the idea that the cAR1 activation also recruits inhibitors to the membrane to shut down signals from free Gβγ to Ras activation. Our computational model is able to simulate the observed spatiotemporal dynamics of known components in adaptation and in gradient sensing by including these putative inhibitor(s) (Meier-Schellersheim et al., 2006). Therefore, we propose that the inhibition process is performed by these negative regulators acting locally on the PI3K

signaling branch and those on PTEN branch, which act in concert to control the spatiotemporal dynamic of PIP_3 around the cell membrane. Future studies are needed to identify inhibitors involved in the GPCR-mediated chemosensing network.

Materials and methods

Cell lines and live cell imaging

As previously described (Xu et al., 2005), *D. discoideum* cell lines expressing PH_{Crac}-GFP(Xu et al., 2005), PTEN-GFP (Iijima and Devreotes, 2002), PI3K1-GFP (Sasaki et al., 2004), and both Gα2CFP and YFPGβ (Xu et al., 2005); and *pten*$^-$, gα1$^-$ and gα9$^-$ cells expressing PH_{Crac}-GFP were developed to the chemotactic stage. Cells were plated on a 1-well chamber for the microinjector delivered cAMP stimulation (Nalge Nunc International), allowed to adhere to the cover glass for 10 min, and then covered with additional DB buffer. Live cells were imaged using a Zeiss Laser Scanning Microscope, LSM 510 META, with a 40× NA 1.3 DIC Plan-Neofluar objective. To monitor cAMP and PH_{Crac}-GFP, PTEN-GFP, PI3K1-GFP cells were excited with two laser lines, 488 nm for GFP and 543 nm for Alexa 594, a water-soluble fluorescence dye. Images were simultaneously recorded in three channels. Channel one: fluorescent emissions from 505–530 nm for GFP (green); channel two: emissions from 580–650 nm for Alexa 594 (red).

Generation and measurement of applied cAMP stimulations

The temporal-spatial intensity changes of Alexa 594 and cells expressing PH_{Crac}-GFP, PTEN-GFP, or PI3K1-GFP were directly imaged using a confocal microscope with Z-axis resolution of ~2 μm. Fluorescence intensities of Alexa 594 and GFP within the focal plane were simultaneously recorded in two different channels. To establish a steady gradient, we set an external supply pressure to 70 hPa (Femtojet and micromanipulator 5171; Eppendorf) to ensure the injection of a constant and small volume of cAMP and Alxea 594 into a one well chamber. Under this condition, a stable gradient was established within 100 μm around the tip of the micropipette. To suddenly expose a cell to a stable gradient, a micropipette filled with a mixture of cAMP and 0.1 g/μl Alexa 594 linked to a FemtoJet was positioned 1,000 μm away from the cells, and then was quickly moved to a position within 100 μm to the cells. During the experiments, we only changed the distance between the micropipette and the cells. The speed of the movement determines how fast a stable gradient can form around a cell (Xu et al., 2005). To withdrawal a gradient, the micropipette was quickly moved away from a cell.

FRET measurement

Using a spectral confocal fluorescence microscope (LSM510 META), we measured intensity decrease of acceptor (YFP) and increase of donor (CFP) in response to stimuli. We monitored intensity changes of CFP (donor) and (YFP) acceptor following a stimulation using a time-lapse acquisition of Lambda Stacks. The cells were excited with a 454-nm laser line and the spectral emissions in each pixel of the fluorescence images were simultaneously recorded in 8 channels, each with a 10-nm width, from 464 to 544 nm. To separate multi-fluorescence signals, each of the fluorescence images was collected using Lambda Stack acquisition. The spectral emissions of fluorescence images were simultaneously recorded in a CHS-1 from 464 nm to 544 nm. The spectra of the cells expressing CFP, YFP or GFP only were obtained and used as the references for the Linear Unmixing Function. The digitally separated images of CFP and YFP of the G cells, and GFP of the PH cells were obtained. The intensities of each fluorophore in the regions of interest in the time-lapse experiments were measured, normalized, and expressed as a function of time in responses to cAMP stimulations, using the software of LSM510 META (Xu et al., 2005).

Imaging and data processing

Images were processed and analyzed by the LSM 510 META software, and converted to TIFF files by the Adobe Photoshop software. All frames of any given series were processed identically. Selected frames of the series were assembled as montages using Photoshop 7.0. Quantification of fluorescence intensities of Alexa 594, GFP, CFP, and YFP in the regions of interest was performed using the LSM 510 META software.

Online supplemental material

Fig. S1 shows inverted PIP_3 responses. Fig. S2 shows FRET measurement of G protein dissociation and association and redissociation. Fig. S3 shows reapplied a cAMP gradient induced an inverted PH_{Crac}-GFP membrane translocation. Fig. S4 A shows Gα9 null cells detect cAMP gradient normally. Fig. S4 B and C show kinetics of the formation the asymmetrically distributed inhibition. Fig. S5 shows PI3K activity, membrane-bound PTEN and the resulting dynamics of PIP_3 in a cell when it is exposed to a cAMP gradient in a computer simulation and a schematic representation of the signaling network that describes spatiotemporal changes. Videos 1 and 2 show uniformly applied cAMP stimulation triggered inverted PH_{Crac}-GFP translocation. Video 3 shows simultaneously measurement of G protein activation in the front and back of a cell and the inverted PH_{Crac}-GFP response. Video 4 shows dynamics of PTEN in a cell upon a withdrawal of a cAMP gradient and then reapplied the gradient. Videos 5 and 6 show a cAMP gradient induced the inverted PH_{Crac}-GFP membrane translocation. Online supplemental material is available at http://www.jcb.org/cgi/content/full/jcb.200611096/DC1.

We thank P. Devreotes and R. Firtel for contributing cell lines to the *Dictyostelium* stock center and J. Brozostowski for gα9$^-$ cells expressing PH_{Crac}-GFP. We thank D. Hereld, A. Kimmel, J. Brozostowski, S. Ou, and X. Xiang for critical comments; and S. Pierce and R. Germain for support.

This study is supported by NIAID/NIH intramural funds.

Submitted: 16 November 2006
Accepted: 6 June 2007

References

Arrieumerlou, C., and T. Meyer. 2005. A local coupling model and compass parameter for eukaryotic chemotaxis. *Dev. Cell.* 8:215–227.

Bominaar, A.A., and P.J. Van Haastert. 1993. Chemotactic antagonists of cAMP inhibit *Dictyostelium* phospholipase C. *J. Cell Sci.* 104:181–185.

Brzostowski, J.A., C.A. Parent, and A.R. Kimmel. 2004. A G alpha-dependent pathway that antagonizes multiple chemoattractant responses that regulate directional cell movement. *Genes Dev.* 18:805–815.

Charest, P.G., and R.A. Firtel. 2006. Feedback signaling controls leading-edge formation during chemotaxis. *Curr. Opin. Genet. Dev.* 16:339–347.

Chung, C.Y., S. Funamoto, and R.A. Firtel. 2001a. Signaling pathways controlling cell polarity and chemotaxis. *Trends Biochem. Sci.* 26:557–566.

Chung, C.Y., G. Potikyan, and R.A. Firtel. 2001b. Control of cell polarity and chemotaxis by Akt/PKB and PI3 kinase through the regulation of PAKa. *Mol. Cell.* 7:937–947.

Comer, F.I., and C.A. Parent. 2002. PI 3-kinases and PTEN: how opposites chemoattract. *Cell.* 109:541–544.

Comer, F.I., C.K. Lippincott, J.J. Masbad, and C.A. Parent. 2005. The PI3K-mediated activation of CRAC independently regulates adenylyl cyclase activation and chemotaxis. *Curr. Biol.* 15:134–139.

Condeelis, J., R.H. Singer, and J.E. Segall. 2005. The great escape: when cancer cells hijack the genes for chemotaxis and motility. *Annu. Rev. Cell Dev. Biol.* 21:695–718.

Devreotes, P.N. 1994. G protein-linked signaling pathways control the developmental program of *Dictyostelium*. *Neuron.* 12:235–241.

Devreotes, P., and C. Janetopoulos. 2003. Eukaryotic chemotaxis: distinctions between directional sensing and polarization. *J. Biol. Chem.* 278:20445–20448.

Devreotes, P.N., and T.L. Steck. 1979. Cyclic 3′,5′ AMP relay in *Dictyostelium discoideum*. II. Requirements for the initiation and termination of the response. *J. Cell Biol.* 80:300–309.

Devreotes, P.N., and S.H. Zigmond. 1988. Chemotaxis in eukaryotic cells: a focus on leukocytes and *Dictyostelium*. *Annu. Rev. Cell Biol.* 4:649–686.

Dinauer, M.C., T.L. Steck, and P.N. Devreotes. 1980a. Cyclic 3′,5′-AMP relay in *Dictyostelium discoideum* IV. Recovery of the cAMP signaling response after adaptation to cAMP. *J. Cell Biol.* 86:545–553.

Dinauer, M.C., T.L. Steck, and P.N. Devreotes. 1980b. Cyclic 3′,5′-AMP relay in *Dictyostelium discoideum* V. Adaptation of the cAMP signaling response during cAMP stimulation. *J. Cell Biol.* 86:554–561.

Funamoto, S., K. Milan, R. Meili, and R.A. Firtel. 2001. Role of phosphatidylinositol 3′ kinase and a downstream pleckstrin homology domain-containing protein in controlling chemotaxis in *Dictyostelium*. *J. Cell Biol.* 153:795–810.

Funamoto, S., R. Meili, S. Lee, L. Parry, and R.A. Firtel. 2002. Spatial and temporal regulation of 3-phosphoinositides by PI 3-kinase and PTEN mediates chemotaxis. *Cell.* 109:611–623.

Gerisch, G. 1982. Chemotaxis in *Dictyostelium*. *Annu. Rev. Physiol.* 44:535–552.

Iglesias, P.A., and A. Levchenko. 2002. Modeling the cell's guidance system. *Sci. STKE.* 2002:RE12.

Iijima, M., and P. Devreotes. 2002. Tumor suppressor PTEN mediates sensing of chemoattractant gradients. *Cell.* 109:599–610.

Iijima, M., Y.E. Huang, and P. Devreotes. 2002. Temporal and spatial regulation of chemotaxis. *Dev. Cell.* 3:469–478.

Janetopoulos, C., T. Jin, and P. Devreotes. 2001. Receptor-mediated activation of heterotrimeric G-proteins in living cells. *Science.* 291:2408–2411.

Janetopoulos, C., L. Ma, P.N. Devreotes, and P.A. Iglesias. 2004. Chemoattractant-induced phosphatidylinositol 3,4,5-trisphosphate accumulation is spatially amplified and adapts, independent of the actin cytoskeleton. *Proc. Natl. Acad. Sci. USA.* 101:8951–8956.

Jin, T., N. Zhang, Y. Long, C.A. Parent, and P.N. Devreotes. 2000. Localization of the G protein betagamma complex in living cells during chemotaxis. *Science.* 287:1034–1036.

Levchenko, A., and P.A. Iglesias. 2002. Models of eukaryotic gradient sensing: application to chemotaxis of amoebae and neutrophils. *Biophys. J.* 82:50–63.

Levine, H., D.A. Kessler, and W.J. Rappel. 2006. Directional sensing in eukaryotic chemotaxis: a balanced inactivation model. *Proc. Natl. Acad. Sci. USA.* 103:9761–9766.

Li, Z., H. Jiang, W. Xie, Z. Zhang, A.V. Smrcka, and D. Wu. 2000. Roles of PLC-beta2 and -beta3 and PI3Kgamma in chemoattractant-mediated signal transduction. *Science.* 287:1046–1049.

Li, Z., X. Dong, Z. Wang, W. Liu, N. Deng, Y. Ding, L. Tang, T. Hla, R. Zeng, L. Li, and D. Wu. 2005. Regulation of PTEN by Rho small GTPases. *Nat. Cell Biol.* 7:399–404.

Lockyer, P.J., S. Wennstrom, S. Kupzig, K. Venkateswarlu, J. Downward, and P.J. Cullen. 1999. Identification of the ras GTPase-activating protein GAP1(m) as a phosphatidylinositol-3,4,5-trisphosphate-binding protein in vivo. *Curr. Biol.* 9:265–268.

Lodowski, D.T., J.A. Pitcher, W.D. Capel, R.J. Lefkowitz, and J.J. Tesmer. 2003. Keeping G proteins at bay: a complex between G protein-coupled receptor kinase 2 and Gbetagamma. *Science.* 300:1256–1262.

Meier-Schellersheim, M., X. Xu, B. Angermann, E.J. Kunkel, T. Jin, and R.N. Germain. 2006. Key role of local regulation in chemosensing revealed by a new molecular interaction-based modeling method. *PLoS Comput. Biol.* 2:e82.

Meili, R., C. Ellsworth, S. Lee, T.B. Reddy, H. Ma, and R.A. Firtel. 1999. Chemoattractant-mediated transient activation and membrane localization of Akt/PKB is required for efficient chemotaxis to cAMP in *Dictyostelium*. *EMBO J.* 18:2092–2105.

Meinhardt, H. 1999. Orientation of chemotactic cells and growth cones: models and mechanisms. *J. Cell Sci.* 112:2867–2874.

Murphy, P.M. 1994. The molecular biology of leukocyte chemoattractant receptors. *Annu. Rev. Immunol.* 12:593–633.

Parent, C.A., and P.N. Devreotes. 1999. A cell's sense of direction. *Science.* 284:765–770.

Parent, C.A., B.J. Blacklock, W.M. Froehlich, D.B. Murphy, and P.N. Devreotes. 1998. G protein signaling events are activated at the leading edge of chemotactic cells. *Cell.* 95:81–91.

Pollard, T.D., and G.G. Borisy. 2003. Cellular motility driven by assembly and disassembly of actin filaments. *Cell.* 112:453–465.

Postma, M., and P.J. Van Haastert. 2001. A diffusion-translocation model for gradient sensing by chemotactic cells. *Biophys. J.* 81:1314–1323.

Postma, M., J. Roelofs, J. Goedhart, H.M. Loovers, A.J. Visser, and P.J. Van Haastert. 2004. Sensitization of *Dictyostelium* chemotaxis by phosphoinositide-3-kinase-mediated self-organizing signalling patches. *J. Cell Sci.* 117:2925–2935.

Sasaki, A.T., C. Chun, K. Takeda, and R.A. Firtel. 2004. Localized Ras signaling at the leading edge regulates PI3K, cell polarity, and directional cell movement. *J. Cell Biol.* 167:505–518.

Servant, G., O.D. Weiner, P. Herzmark, T. Balla, J.W. Sedat, and H.R. Bourne. 2000. Polarization of chemoattractant receptor signaling during neutrophil chemotaxis. *Science.* 287:1037–1040.

Stephens, L., C. Ellson, and P. Hawkins. 2002. Roles of PI3Ks in leukocyte chemotaxis and phagocytosis. *Curr. Opin. Cell Biol.* 14:203–213.

Ueda, M., Y. Sako, T. Tanaka, P. Devreotes, and T. Yanagida. 2001. Single-molecule analysis of chemotactic signaling in *Dictyostelium* cells. *Science.* 294:864–867.

Van Haastert, P.J., and P.N. Devreotes. 2004. Chemotaxis: signalling the way forward. *Nat. Rev. Mol. Cell Biol.* 5:626–634.

Wessels, D., R. Brincks, S. Kuhl, V. Stepanovic, K.J. Daniels, G. Weeks, C.J. Lim, G. Spiegelman, D. Fuller, N. Iranfar, et al. 2004. RasC plays a role in transduction of temporal gradient information in the cyclic-AMP wave of *Dictyostelium discoideum*. *Eukaryot. Cell.* 3:646–662.

Xu, J., F. Wang, A. Van Keymeulen, P. Herzmark, A. Straight, K. Kelly, Y. Takuwa, N. Sugimoto, T. Mitchison, and H.R. Bourne. 2003. Divergent signals and cytoskeletal assemblies regulate self-organizing polarity in neutrophils. *Cell.* 114:201–214.

Xu, X., M. Meier-Schellersheim, X. Jiao, L.E. Nelson, and T. Jin. 2005. Quantitative imaging of single live cells reveals spatiotemporal dynamics of multistep signaling events of chemoattractant gradient sensing in *Dictyostelium*. *Mol. Biol. Cell.* 16:676–688.

Zigmond, S.H. 1978. Chemotaxis by polymorphonuclear leukocytes. *J. Cell Biol.* 77:269–287.